THE JOURNAL OF BIOLOGICAL CHEMISTRY
Vol. 277, No. 41, Issue of October 11, pp. 38838–38846, 2002
Printed in U.S.A.

Modulation of Hepatitis C Virus RNA-dependent RNA Polymerase Activity by Structure-based Site-directed Mutagenesis*

Received for publication, May 13, 2002, and in revised form, July 16, 2002
Published, JBC Papers in Press, July 26, 2002, DOI 10.1074/jbc.M204657200

Patrick Labonté‡, Vladimir Axelrod‡, Atul Agarwal§, Ann Aulabaugh§, Anthony Amin‡, and Paul Mak‡¶

From the ‡Department of Infectious Disease and §Department of Biological Chemistry, Wyeth, Pearl River, New York 10965

The hepatitis C virus (HCV) encodes an RNA-dependent RNA polymerase (NS5B), which is indispensable for the viral genome replication. Although structural comparison among HCV NS5B, poliovirus 3D-pol, and human immunodeficiency virus-reverse transcriptase RNA-dependent polymerase reveals the canonical palm, fingers, and thumb domains, the crystal structure of HCV NS5B highlights the presence of a unique A1-loop, which extends from the fingers to the thumb domain (amino acids 12–46), providing many contact points for the proposed "closed" conformation of the enzyme. The polymerase also possesses a tunnel, which starts at the active site and terminates on the back surface of the enzyme. This tunnel of 19 Å contains five basic amino acids, which may be engaged in NTP trafficking. In the present study, we exploited the crystal structure of the enzyme to elucidate the involvement of these two structural motifs in enzyme activity by site-directed mutagenesis. As predicted, the replacement of leucine 30 located in the Λ1-loop is detrimental to the NS5B activity. Heparin-Sepharose column chromatography and analytical ultracentrifugation experiments strongly suggest a local alteration in the structure of the Leu-30 mutant. An analysis of amino acid substitutions in Arg-222 and Lys-151 within the putative NTP tunnel indicates that Arg-222 was critical in delivering NTPs to the active site, whereas Lys-151 was dispensable. Interestingly, the substitution of lysine 151 for a glutamic acid resulted in an enzyme that was consistently more active in *de novo* synthesis as well as by "copy-back" mechanism of a self-primed substrate when compared with the wild type NS5B enzyme. Burst kinetic analyses indicate that the gain in function of K151E enzyme was primarily the result of the formation of more productive preinitiation complexes that were used for the elongation reaction. In contrast to the recent observations, both the wild type and mutant enzymes were monomeric in solution, whereas molecules of higher order were apparent in the presence of RNA template.

Hepatitis C virus (HCV)[1] is the major etiological agent of non-A non-B hepatitis and infects an estimated 3% of the world's population (1). Approximately 80% of the infected individuals will remain chronically infected for decades and may eventually develop severe liver cirrhosis and hepatocellular carcinoma (2). In the absence of a prophylactic vaccine or a specific antiviral agent, the best treatment currently available for HCV infection is the combination therapy of interferon and ribavirin (3).

HCV is an enveloped virus belonging to the hepacivirus gender in the Flaviviridae family, which also includes the flavivirus and pestivirus (4). The single-stranded positive-sense RNA genome is ~9.5 kb in length and produces a single polyprotein of 3010–3040 amino acids (5). The polyprotein is processed by a combination of viral and cellular proteases, giving rise to at least 10 individual proteins (6). In the absence of a permissive cell culture replication system, the knowledge of HCV replication has been derived mainly from alternative *in vitro* systems or from the biochemical characterization of individual viral proteins (7–11). Among these viral proteins, the HCV polymerase (NS5B), which is an RNA-dependent RNA polymerase (RdRP), has been investigated extensively because it is the prime-target for the development of antiviral drug (12–15). HCV polymerase activity was first reported using self-priming mechanism (copy-back) in which the RNA folds back intramolecularly. However, copy-back replication is rather nonspecific and is unlikely to be used by the virus *in vivo* (16). More recently, RNA replication by HCV NS5B has been reported by *de novo* synthesis (17–19), which has also been reported for other viral polymerases including the bacteriophage $\phi 6$, Qβ, the brome mosaic virus, and the bovine viral diarrhea virus (20–25). *De novo* RNA synthesis appears to be an attractive model for viral RNA replication because no genetic information is lost during the replication. Furthermore, no additional enzymes are needed to generate the primer or to cleave the region between template and newly synthesized RNA. However, *de novo* initiation of RNA synthesis is relatively inefficient *in vitro* and requires very high concentrations of GTP, which is the initiating nucleotide incorporated into the template.

With the recent resolution of the NS5B crystal structure (26, 27), certain unique structural elements of the enzyme have been highlighted (see Fig. 1). Although the canonical palm, fingers and thumb domains as well as the putative NTP tunnel are well conserved among HCV NS5B, poliovirus 3D-pol, and human immunodeficiency virus-reverse transcriptase enzymes, the space between the fingers and the thumb domains of NS5B is unexpectedly small, giving rise to a proposed "closed" conformation, which has also been identified for the double-stranded RNA polymerase of $\phi 6$ (28). Based on their crystal structures, both enzymes possess a loop that connects the fingers with the thumb. This loop, previously called Λ1 on the HCV NS5B structure, could be the major element respon-

* This work was supported by the postdoctoral program at Wyeth-Discovery. The costs of publication of this article were defrayed in part by the payment of page charges. This article must therefore be hereby marked "*advertisement*" in accordance with 18 U.S.C. Section 1734 solely to indicate this fact.

¶ To whom correspondence should be addressed. Present address: Wyeth Research, 85 Bolton St., R231A, Cambridge, MA 02140. Tel.: 617-665-8934; E-mail: makp@wyeth.com.

[1] The abbreviations used are: HCV, hepatitis C virus; DTT, dithiothreitol; BSA, bovine serum albumin; RdRP, RNA-dependent RNA polymerase; wt, wild type; HS, heparin-Sepharose.

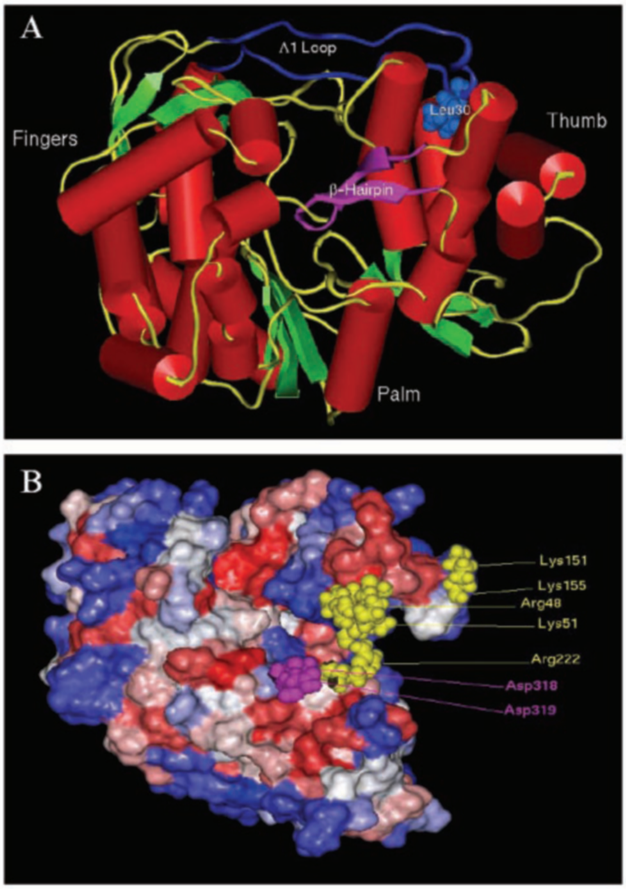

FIG. 1. **Crystal structure of the HCV polymerase (NS5B).** *A*, front view of the HCV polymerase representation of the palm, fingers, and thumb domains. α-Helices are shown as *red cylinders*, β-strands as *green arrows*, and connecting loops as *yellow* and *blue tubes*. The back of the enzyme is closed by the Λ1-loop (*blue tube*) that emanates from the fingers to make contact points with the thumb. Leucine 30 (*blue*) is predicated to anchor the Λ1-loop to the thumb domain via strong hydrophobic interaction. The β-hairpin, which is positioned over the active site is shown in *pink*. *B*, right side view of the protein with emphasis on the NTP tunnel. The thumb domain has been removed for clarity. Positively charged amino acids engaged in the NTP tunnel are indicated in *yellow* (Lys-151, Lys-155, Arg-48, Leu-51, and Arg-222). The aspartic acids 318 and 319 in *pink* are located in the active site.

sible for the closed conformation of HCV NS5B and φ6 polymerase and might play a key role in the "clamping" motion of these enzymes. Another interesting feature of the HCV polymerase is the presence of a β-hairpin that hangs over the active site. Although the function of this unique structure is unclear, it has been suggested that the β-hairpin may function as a gate to position the very 3′-end of the RNA at the active site (29). Crystal structure of the enzyme indicates that the space underneath the β-hairpin is not sufficient to allow the passage of a double stranded-RNA structure. Therefore, the β-hairpin should exhibit the flexibility to move to accommodate the elongation of the nascent double-stranded RNA. The NTP tunnel is a common structural motif observed for RNA-dependent polymerases. Although it is logical to hypothesize that the negatively charged incoming NTPs interact sequentially with positively charged amino acids to reach the active site within the NTP tunnel, systematic analysis of the nucleotide involvement in such trafficking has not been examined.

In this study, we exploited the crystal structure of the HCV NS5B polymerase to analyze the involvement of specific residues on the overall RdRP activity. To delineate whether the Λ1-loop is involved in keeping the enzyme in a "closed" conformation, we mutated leucine 30, which exhibits strong hydrophobic interaction with the thumb domain to polar residues (an arginine or a serine). Furthermore, the role of the basic amino acids in NTP trafficking was analyzed by mutating the last positively charged amino acid (arginine 222) in close proximity to the active site and the first amino acid (lysine 151) located at the beginning of the NTP tunnel. Our data indicate that most of these point mutations modulate the NS5B activity and the Λ1-loop is a critical element in determining the activity of the enzyme. More interestingly, real-time analytical ultracentrifugation analyses demonstrated that both the wild type and mutant enzymes are monomeric in solution, whereas oligomeric forms of the enzymes can be induced by short RNA template binding.

MATERIALS AND METHODS

Protein Expression and Purification—The HCV NS5B protein (HCV-BK) lacking the 21 C-terminal amino acids was expressed in pET-24b containing a C-terminal hexahistidine tag. All single point mutations were derived from the pET-24b/NS5B plasmid using the QuikChange™ site-directed mutagenesis kit (Stratagene). Protein production from *Escherichia coli*, BL21(DE3) was induced by adding isopropyl-β-D-thiogalactoside to a final concentration of 1 mM. Cell pellets were resuspended in lysis buffer containing 20 mM Tris-HCl (pH 7.4), 500 mM NaCl, 1 mM 2-mercaptoethanol, 30 mM imidazole, 2.5% glycerol, EDTA-free protease inhibitor tablets (Roche Molecular Biochemicals) and passed through a French press apparatus (25,000 p.s.i.; three times). The cytosolic fraction after centrifugation (35,000 rpm for 30 min; SA600 rotor) was applied to a nickel column (Superflow, Qiagen). After washing with lysis buffer, the protein was eluted from the column with a lysis buffer containing 350 mM NaCl and 200 mM imidazole. The eluted protein was then applied to a HiTrap™ heparin column (Amersham Biosciences) and subsequently washed with a buffer containing 20 mM Tris-HCl (pH 7.4), 350 mM NaCl, 10 mM DTT, and 2.5% glycerol. Protein was eluted from the column with a linear gradient of NaCl (350–900 mM). After an overnight dialysis against a buffer containing 50 mM Tris-HCl (pH 7.4), 300 mM NaCl, 10 mM DTT, and 50% glycerol, the protein was aliquoted and stored at −70 °C. Stock enzyme was tested for the presence of contaminating RNase using RNaseAlert™ (Ambion).

Sucrose Gradient Centrifugation—To analyze the biophysical state of the wild type enzyme and some of the substitution variants, 6 μg of NS5B enzyme or 20 μg of BSA were loaded on top of a sucrose step gradient (2 ml) containing 10, 20, 25, 30, and 35% of sucrose in 20 mM HEPES (pH 7.5), 50 mM NaCl, and 1 mM DTT. Gradients were centrifuged at 85,000 × *g* for 24 h. Fractions were collected using the Auto Densi-Flow™ IIC collector (Buchler Instruments) and subsequently analyzed on SDS-PAGE. Proteins were detected by the Silver Stain Plus detection kit (Bio-Rad). The sucrose concentration of each fraction was determined using the ABBE-3L refractometer (Milton Roy).

Analytical Ultracentrifugation—Samples were prepared in 20 mM Trizma (Tris base), 500 mM sodium chloride, and 3% glycerol at pH 7.5 to a final concentration of 1 μM protein. Samples containing RNA were adjusted to 500 mM in sodium chloride to reduce nonspecific RNA-protein interactions. The partial specific volume of the proteins was calculated based on the amino acid composition, and the density of the solvent was calculated from the chemical composition of the buffer using the computer program SEDNTERP and adjusted for temperature. Sedimentation velocity experiments were performed on a Beckman model XLI/XLA analytical ultracentrifuge operating at a rotor speed of 35,000 rpm and 20 °C using 390 μl loaded into two-channel carbon-Epon centerpieces in an An-Ti 60 rotor. Data were collected in continuous mode, at a single wavelength (280 nm) with a step size of 0.006 cm without signal averaging. Multiple scans at different time points were fitted to a continuous size distribution using the program SEDFIT (30).

"Copy-back" RNA Synthesis—To measure the polymerase activity of the NS5B mutants, a 369-nucleotide RNA called pOF was used as a template. The sequence of this substrate is 5′-GAAUACAAGCUUGG-GCUGCAGGUCGACUCUAGAGGAUCCCCGGGCGCUAGGAACAC-UCAGGAUCACGUUCGCUCUCUGUGCCUUUUAGCUUGGCACAA-UGGCGAAGAAGAAUAUAACAAAUUCCUAGCUAAAAUCAGGAGU-GUGCCAAUUGGAAGAGCUUUAUUGCUCCCAGAGUACUCAACA-UUGUACCGCCGUUGGCUUGACUCAUUUUAGUAACCCUACCUC-AGUCGAAUUGGAUUGGGUCAUACUGUUGUAGGGGUAAAUUU-UUCUUUAAUUCGGAGAAAAAAAAAAAAAAAAAAAAAAAAAAAAA-AAAAAAAAAAAAAAAAAAAAAAAAAAAAAAAAAAAAAAAAAA-

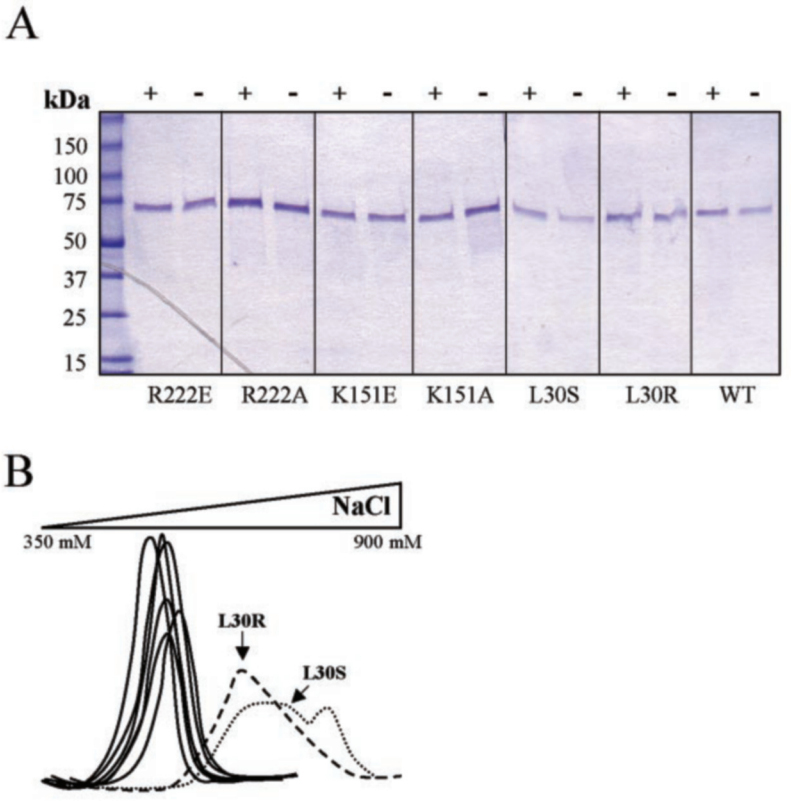

FIG. 2. **Purification and biophysical analysis of HCV NS5B mutants.** *A*, purified NS5B mutants were analyzed for the presence of residual protease contaminant. Each mutant (500 ng) was incubated for 2 h on ice (−) or at 37 °C (+) prior to SDS-PAGE analysis. Proteins were stained with Coomassie Blue. *B*, elution profile of NS5B mutants on heparin-Sepharose column. Proteins were eluted simultaneously with a gradient of sodium chloride (350–900 mM) using a multistaltic pump (HBI).

AAAAAAAAAAAGAAUU-3′. The standard nucleotide incorporation reaction was performed as described below unless indicated otherwise in the figure legend. Reactions were performed in a volume of 50 μl containing 20 mM HEPES (pH 7.5), 5 mM $MgCl_2$, 1 mM DTT, 20 nM NS5B enzyme, 20 nM pOF, 20 units of RNasin, 50 μg/ml BSA, 100 μM UTP, CTP, and ATP, 5 μM GTP, and 2.5 μCi of [α-^{33}P]GTP. Reactions were incubated at 37 °C for 90 min and stopped by addition of 10 μl of 0.5 M EDTA. The reaction mixture was filtered through a 96-well plate DEAE filter paper (Millipore) and washed (five times) with 200 μl of 0.5 M sodium phosphate buffer (pH 7.0). The plates were air-dried for 10 min, and 50 μl of Scintisafe Plus™ 50% (Fisher Scientific) was added for scintillation counting using a β-counter (Wallac).

Burst Assay—The pOF RNA was used as a template for the burst experiment. Briefly, 40 nM enzyme was pre-incubated with 40 nM pOF RNA for 4 h at room temperature in a buffer containing 20 mM HEPES (pH 7.5), 10 mM $MgCl_2$, 2 mM DTT, 100 μg/ml BSA, and 20 units of RNasin (final volume: 25 μl). At the end of the pre-incubation period, the reaction was incubated at 37 °C for 5 min and subsequently initiated by the addition of 25 μl of a pre-heated buffer (37 °C) containing 20 mM HEPES (pH 7.5), 800 ng/ml heparin, 100 μM CTP, ATP, and UTP, 5 μM GTP, and 2.5 μCi of [α-^{33}P]GTP. At each end point, the reaction was stopped by addition of 10 μl of 0.5 M EDTA. For gel analysis of the burst experiment, the same procedure was performed except that the reactions were stopped by addition of an equal volume of phenol:chloroform (1:1). After protein extraction, the labeled RNA was ethanol-precipitated in the presence of 3 M sodium acetate (pH 5.0) and 20 μg of glycogen. RNA was resuspended in 20 μl of glyoxal loading buffer (Ambion) and resolved in a 2.5% agarose gel.

Nucleotide Incorporation Using Homopolymeric Template and Dinucleotide Primer—All four homopolymeric templates (poly(U), -(A), -(C), and -(G)) were purchased from Sigma. The dinucleotide primers synthesized with a 5′-phosphate (pGG, pCC, pUU, and pAA) were purchased from Oligo Etc. (Wilsonville, OR). For standard experiments, a 50-μl reaction was performed using 20 nM enzyme, 20 nM homopolymeric template, and 15 μM complementary dinucleotide primer pGG, pAA, or pCC or 80 μM pUU. The reaction was performed essentially in the same reaction condition as for the copy-back RNA synthesis, except that the respective nucleotides were used at 100 μM.

De Novo Initiation of Elongation Using Homopolymeric Template—Under our conditions, the initiation of *de novo* synthesis by the NS5B mutants was observed only for poly(C) homopolymeric template but not poly(A), poly(U), or poly(G). To determine the K_m and V_{max} values, reactions were performed in quadruplicate using 20 nM enzyme, 20 nM poly(C), and 0–2.0 mM GTP under the same reaction conditions as for the copy-back RNA synthesis.

De Novo Single Nucleotide Incorporation—To examine the incorporation of the third and fourth nucleotides following a *de novo* initiation, a 23-mer RNA (5′-AAAAAAAAAAAAAAAAACAGUCC-3′) was used as a template. The reaction was performed in a 50-μl volume containing 20 mM HEPES (pH 7.5), 5 mM $MgCl_2$, 1 mM DTT, 250 nM NS5B enzyme, 250 nM 23-mer template, 20 units of RNasin, 50 μg/ml BSA, 1 mM GTP, and 25 μCi of [α-^{33}P]ATP or 100 μM ATP and 25 μCi of [α-^{33}P]CTP. The reaction was incubated at 37 °C for 0–10 min and stopped by addition of an equal volume of phenol chloroform. After protein extraction, the labeled RNA was ethanol-precipitated in the presence of 3.0 M sodium acetate (pH 5.0) and 20 μg of glycogen. RNA was resuspended in 4 μl of TBE-urea sample buffer (Novex) and resolved on a 25% TBE-urea acrylamide gel.

RESULTS

Expression and Purification of the HCV NS5B Mutants—The wild type and amino acid substituted variants of NS5B enzyme were purified to near homogeneity (>90%) by sequential chromatography using a nickel and a heparin-Sepharose (HS) column, respectively, as described under "Materials and Methods" (Fig. 2*A*). Analysis of these preparations showed that they did not contain any contaminating protease or RNase activities (Fig. 2*A* and data not shown). Tracing of the salt elution profile of the enzyme from HS column indicated that the wild type enzyme and most of the variant NS5B proteins eluted at ~400 mM sodium chloride (Fig. 2*B*). Interestingly, two point mutants containing the L30R and L30S substitutions, respectively, were eluted at a higher salt concentration (600 mM NaCl) from the HS column. The biophysical state of the NS5B wild type and point mutant proteins was analyzed by sucrose gradient centrifugation, which indicated that the sedimentation profiles were similar to that of the bovine serum albumin protein (data not shown). This observation suggests that the proteins were likely monomeric in solution. These preparations were subsequently used for biochemical characterization of the enzyme.

Optimization of Enzyme Assay Using a Self-primed Copy-

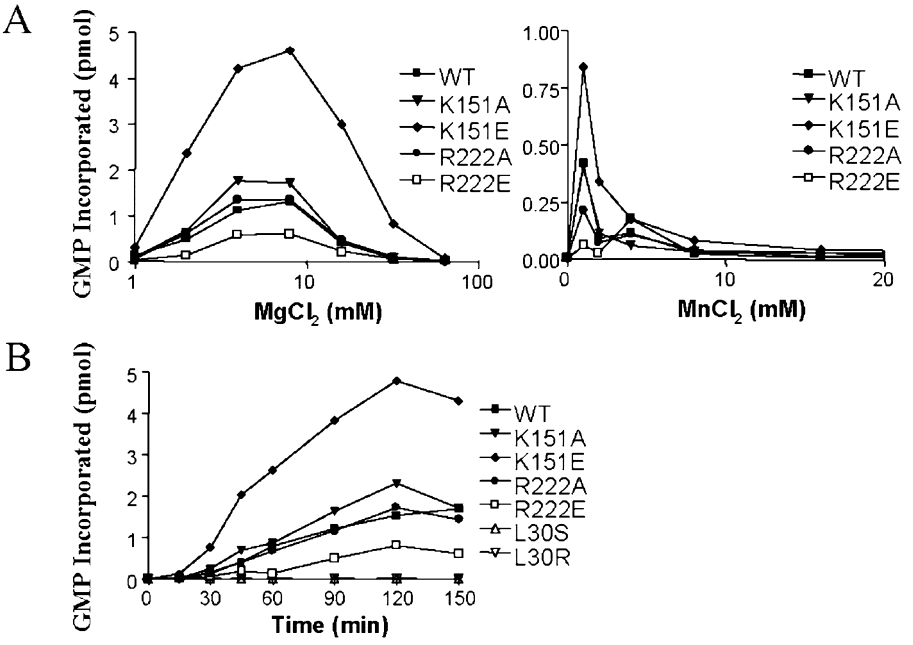

FIG. 3. **Characterization of NS5B mutants using a self-priming template.** *A*, effect of divalent cations ($MgCl_2$ and $MnCl_2$) on enzyme activity. The reaction was conducted at 37 °C for 90 min using 20 nM each of enzyme and pOF in the presence of $MgCl_2$ or $MnCl_2$ as indicated. *B*, time course of enzyme activity. The enzyme and pOF substrate were used at 20 nM each with 5 mM $MgCl_2$ at 37 °C. The reaction was stopped by adding 10 μl of EDTA (0.5 M), and the GMP incorporation was quantified by DEAE filter binding assay. The data represent the average of quadruplicate experiments.

back RNA Substrate—As described previously, NS5B can utilize an RNA molecule that folds back intramolecularly at the 3′-OH end as a substrate to catalyze complementary strand synthesis resulting in a copy-back double-stranded RNA product (9). For the experiments described herein, the copy-back substrate was a 369-nucleotide RNA derived from the poliovirus 3′-end, pOF. This RNA contains two uridines at the 3′-OH end that can fold back to pair with adenosine residues in an adjoining polyadenosine stretch, which is located four nucleotides upstream of the uridine residues. To optimize the reaction condition, the effects of temperature and divalent cations on the enzyme activity were examined. The enzyme activity was 20-fold higher at 37 °C when compared with 21 °C (data not shown). In contrast to previous reports, the enzyme activity was 4 times higher when magnesium was used as a divalent cation rather than manganese (Fig. 3*A*) (12, 18, 19). Using these optimal conditions (37 °C and 5 mM $MgCl_2$), a titration of each enzyme preparation using 20 nM RNA substrate showed that an enzyme concentration of 20 nM (data not shown) and 90 min of incubation defined the upper linear range for the enzyme (Fig. 3*B*).

Effects of Leu-30 Substitutions on the Enzyme Structure and Activity—The resolved crystal structure of the NS5B enzyme exhibits a "closed" conformation (26, 27). Based on this information, we hypothesized that the unique Λ1-loop shown in Fig. 1*A* is likely engaged in coordinating the movement of the thumb and fingers domains. Within this loop, leucine 30 has multiple interactions with a hydrophobic pocket of the thumb domain (Fig. 1*A*). Perturbation of this hydrophobic pocket could result in local alteration of the loop at the contact sites with the thumb, which might subsequently lead to an "open" conformation of the enzyme. To test this hypothesis, two point mutations were introduced at this location, *i.e.* L30R and L30S. During the chromatography process, these point mutants containing the L30R or L30S substitutions bound to the HS column with higher affinity when compared with the other proteins as reflected by their elution maxima (600 mM NaCl) (see Fig. 2*B*). This altered chromatographic behavior is highly suggestive of a conformational change, which in turn may modify the numbers of charge of these mutants available to interact with the resin (Fig. 2*B*). More importantly, both of these mutant enzymes were inactive in the polymerase assay using pOF as a template

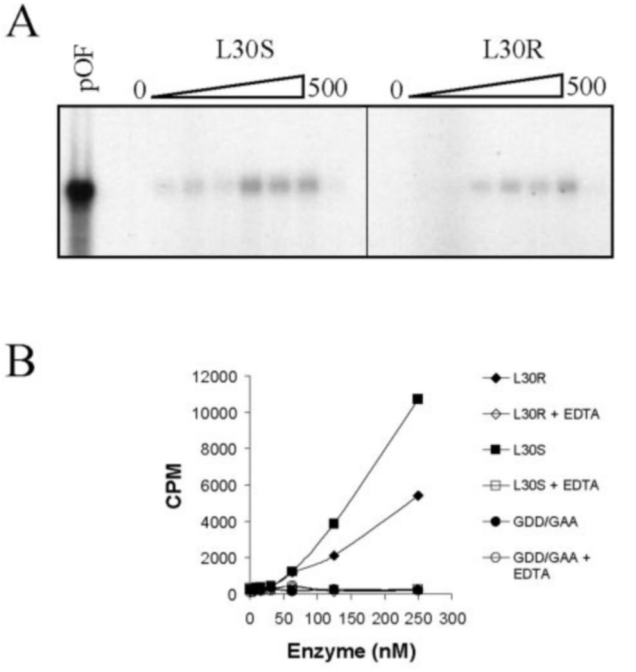

FIG. 4. **Enzyme titration of L30R and L30S using self-priming template (pOF) and [α-^{33}P]UTP as sole source of nucleotide.** *A*, the reaction was performed at 37 °C for 90 min with 20 nM pOF and 5 μCi of [α-^{33}P]UTP with enzyme concentrations ranging from 0 to 500 nM. Control γ-^{33}P-labeled pOF is shown in the *first lane*. Products were resolved on a 2.5% agarose gel. *B*, the experimental protocol is similar to *A* except that the incorporation of [α-^{33}P]UTP was quantified by DEAE filter binding assay. Addition of EDTA to the reaction buffer showed that the incorporation was NS5B-specific.

and [α-^{33}P]GTP as a label (Fig. 3*B*). Nevertheless, very low enzyme activity could be detected when an enzyme titration using [α-^{33}P]UTP as the only source of nucleotide triphosphate was performed (Fig. 4). The basal level of nucleotide incorporation was observed in a dose-dependent manner (Fig. 4*A*) and was NS5B-specific because a "dead" enzyme (GDD/GAA), in which the essential GDD motif had been replaced by GAA did not exhibit any nucleotide incorporation under the same assay conditions (Fig. 4*B*). However, the L30S and L30R mutants

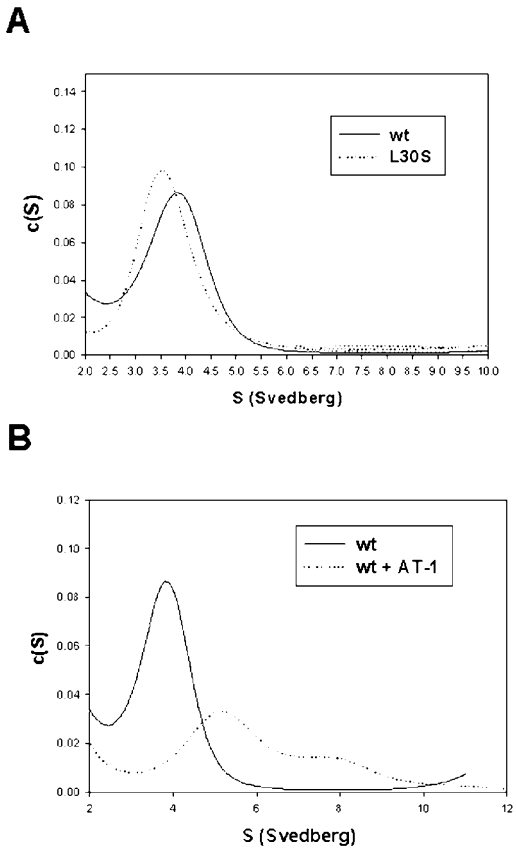

FIG. 5. **Continuous size distribution analysis (analytical ultracentrifugation) of wild type and L30S mutant NS5B polymerase in the absence of RNA template (*A*), or in the presence of RNA template (*B*).** The sequence and structure of the short RNA template (AT-1) is shown in *C*.

incorporated 60 and 66 times less UMP, respectively, when compared with the wt-NS5B (data not shown). To determine whether there is a structural change in the mutant enzyme, the global shape of L30S was compared with that of the wt-enzyme by analytical ultracentrifugation. The results shown in Fig. 5*A* suggest that the global shapes of both enzymes where similar (see below). Taken together, this biophysical analysis and the chromatographic behavior of the L30S mutant support the notion that a rather local structural modification had occurred at the contact sites between the Λ1-loop and the thumb. Because these single amino acid substitutions were detrimental to NS5B activity, we attempted to restore the structure and function of the L30S mutant by inserting compensatory mutations. To this end, serine 29 in the Λ1-loop was replaced by an aspartic acid in an attempt to create an ionic interaction with the arginine 503 of the thumb domain. For the same reason, histidine 428 was replaced by an asparagine to favor the creation of a hydrogen bond with serine 30 of the L30S mutant. Unfortunately, neither of these double mutants (L30S/S29D and L30S/H428N) were compensatory. Indeed, both of these mutants had chromatographic behavior and enzyme activity similar to that of the L30S mutant (data not shown).

TABLE I
Apparent molecular masses of HCV NS5B by analytical ultracentrifugation

Sample[a]	Buffer[b]	Sedimentation coefficient	Apparent molecular mass[c]
			kDa
wt	200 mM NaCl	3.6	64
wt	500 mM NaCl	3.9	65
wt + AT-1	500 mM NaCl	5.2	74.9
	500 mM NaCl	8.0	145
L30S	500 mM NaCl	3.6	64
L30S + AT-1	500 mM NaCl	4.0	78.4
	500 mM NaCl	6.4	155
	500 mM NaCl	9.4	>200

[a] 1 μM protein, 0.5 μM AT-1.
[b] 20 mM Tris, 4% glycerol, and NaCl.
[c] Molecular mass based on amino acid or nucleotide composition: wt, 64,216 Da; L30S, 64,189 Da; AT-1, 8679 Da.

Monomeric and Oligomeric Forms of the wt-NS5B and L30S Enzymes—It has been shown recently that HCV NS5B can form dimers and oligomers in solution and this intrinsic oligomerization of the enzyme is essential for the polymerase activity (31–33). To define the quarternary structure of the wild type and mutant enzymes in the present study, analytical ultracentrifugation was employed to examine these proteins in solution in the presence *or* absence of RNA substrate. As shown in Fig. 5*A*, both wt-NS5B and L30S enzymes had sedimentation coefficients of 3.9 and 3.6 S, respectively, under high ionic strength, consistent with monomeric molecular masses (see Table I). Similar S (Svedberg) values were obtained at low and physiological ionic strength (data not shown). Our data contradict the oligomeric interaction observed in the reported glycerol gradient fractionation (32), although the current study was conducted at low glycerol content (4%). Because the oligomeric state of the enzyme in the presence of an RNA template reflects a more biological phenomenon in the context of directing RNA synthesis, we examined the sedimentation coefficients of the proteins in the presence of a short hairpin RNA template (see Fig. 5*C*). Very similar hairpin loops have been utilized by NS5B enzyme to initiate *de novo* synthesis (17). High ionic strength conditions were employed to reduce nonspecific binding of the RNA with the polymerase. To our surprise, a shift in the S values was observed for both the wt-NS5B and L30S mutant (Fig. 5*B*). In the case of the wt-NS5B, the sedimentation velocity profiles fit well for two species of 5.2 and 8.0 S (Fig. 5*B*). Analysis of the boundary spreading yielded molar masses of 74.9 and 145 kDa, consistent with RNA complexed with monomeric protein (74.9 kDa) or dimeric protein (145 kDa) (Table I). For the L30S mutant, three distinct peaks were observed with S values of 4.0, 6.5, and 9.4 corresponding to monomer, dimer, and potentially tetramer binding to the RNA. Small quantities of 14 S oligomer were also detected. These observations suggest dimerization/oligomerization of HCV NS5B can be induced by RNA binding and that this intrinsic ability of the L30S mutant might be different from the wild type enzyme. These results with the wild type enzyme are consistent with the recent finding which indicates that the NS5B polymerase acts as a functional oligomer (33). Although we used a short hairpin RNA as template, the possibility that two or more monomeric molecules binding to the same RNA cannot be excluded. It is important to note that the hairpin structure of the RNA template is required for RNA-induced oligomerization because NS5B-RNA complex could not be detected when a linear version of the RNA template was used in analytical ultracentrifugation (data not shown). Further experiments are required to address the quaternary structure of the polymerase at the initiation step.

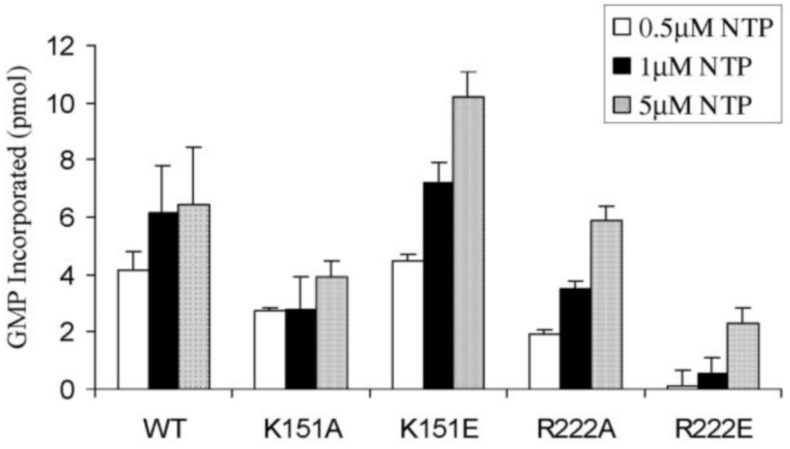

FIG. 6. **Activity of NS5B mutants at low nucleotide concentrations.** In this assay, all four NTPs were adjusted to 0.5, 1, or 5 μM with 20 nM of enzyme and 20 nM pOF and incubated for 90 min at 37 °C. GMP incorporation was determined by DEAE filter binding assay as described previously. The data represent the mean of three separate experiments with the standard error (*bar*).

NTP Tunnel—The HCV NTP tunnel is ~19 Å long and consists of five positively charged amino acids located within the tunnel. We hypothesized that these residues could interact sequentially with the phosphate group of the incoming NTPs to facilitate its entry to the active site of the enzyme (Fig. 1*B*). This notion was tested by mutating the last (arginine 222) and the first (lysine 151) amino acids within the NTP tunnel to alanine and glutamic acid (R222A, R222E and K151A, K151E). In theory, replacement of the positively charged amino acids for negatively charged amino acids within the tunnel could result in charge repulsion of the incoming NTPs leading to an attenuation or abolishment of the polymerase activity. In excess of NTPs, conservative substitution of Arg-222 and Lys-151 (R222A and K151A) had only a subtle effect on polymerase activity (see Fig. 3*B*). Indeed, when the assay was done in excess of NTPs, the R222E mutant exhibited a 50% reduction in activity when compared with the wt-NS5B. Surprisingly, the glutamic acid substitution at amino acid 151 (K151E) did not reduce the activity of the enzyme. In contrast, the K151E mutant exhibited an increase in enzyme activity (Fig. 3*B*) and the enzyme was monomeric in solution as demonstrated by analytical ultracentrifugation (data not shown). Because the polymerase activity was performed in excess of NTPs, it was possible that a sufficient amount of NTPs could get through the tunnel or diffuse to the active site via an alternative path resulting in normal enzyme activity *in vitro*. To address this possibility, the activity of the enzyme was performed at relatively low NTP concentrations. When the four NTPs were supplemented at 0.5 μM, the R222E variant enzyme was inactive in the assay whereas R222A variant was partially active (Fig. 6). This result suggests that the R222E enzyme may not have allowed adequate access of NTPs to the active site at lower concentration of NTPs, supporting the notion that Arg-222 may be essential in NTP trafficking. Lowering of the NTP concentration did not abrogate the K151E activity, which was comparable with that of the wt-NS5B. In fact, a slight increase in NTP concentration enhanced the K151E enzyme activity when compared with the wt-NS5B (Fig. 6).

The K151E Substitution Increases the Overall Enzyme Activity—Enzyme titration experiments showed that the activity of K151E enzyme was 7–10 times higher at 21 °C, and 2–3 times higher at 37 °C than that of the wt-NS5B (data not shown). To determine if the apparent enhancement in enzyme activity is caused by more active enzyme molecules in the protein preparation, or an increase in the polymerization rate or processivity, a burst assay was performed in the presence of heparin, which serves as a trapping agent. After pre-incubation of the enzyme with the pOF template, the reaction was initiated by the addition of NTPs and heparin. Under these conditions, the enzyme molecules that are bound to the substrate will complete only one round of RNA synthesis because they will bind to heparin and cannot engage in another round of synthesis after dissociating from the template. As shown in Fig. 7*A*, all enzymes except K151E incorporated about the same amount of NTPs as quantified by a filter binding assay, suggesting comparable numbers of pre-initiation complex were formed during the pre-incubation period. However, the amount of incorporated NTPs for the K151E mutant was 7 times higher when compared with the wt-NS5B. This observation strongly suggests that K151E enzyme is able to form more pre-initiation complex under these reaction conditions. To evaluate whether the incorporation of NTPs observed by filter binding assay results from processive enzymes, the products of the kinetic burst assays were analyzed by gel chromatography. As shown in Fig. 7*B*, all enzymes were equally processive under these conditions because no truncated intermediate product was observed.

Finally, the rate of elongation was compared between K151E and the wt-NS5B enzymes in a burst kinetic assay followed by gel analysis of products (Fig. 8). When the experiment was performed using [α-^{33}P]GTP as label, the initial velocity of the reaction could not be observed because the first cytidylate on the pOF substrate is located 84 nucleotides away from the 3′ end of the template. Because the template contains a polyadenosine stretch near the self-primed 3′-OH end, [α-^{33}P]UTP was used as an alternative to measure the initial velocity of the reactions in a more accurate fashion. As shown in Fig. 8, there was no difference in enzyme velocity between the wt-NS5B and K151E enzymes, indicating that their rate of elongation is similar.

Enzyme Activity Using Dinucleotide-primed Homopolymeric Templates—It has been recently reported that the HCV polymerase can utilize RNA template primed with a guanosine dinucleotide more efficiently than a self-primed RNA (3) To compare the kinetics for the wt-NS5B and variant enzymes, the efficiency of RNA synthesis was determined using poly(A)/pUU, poly(U)/pAA, poly(G)/pCC, and poly(C)/pGG as template/primers. Under the reaction conditions used in this study, only the poly(C)/pGG and, to a lesser extent, poly(A)/pUU were utilized by the enzymes. As shown in Table II, the kinetic data indicated that the activities of K151E and the wt-NS5B were similar with poly(C)/pGG as template/primer, whereas the K151E enzyme was more active than wt-NS5B when poly(A)/pUU was used (K_{cat}/K_m are 73,913 and 10,066, respectively). Neither R222A nor R222E enzymes were capable of utilizing the poly(A)/pUU as template/primer.

Characterization of the de Novo Synthesis of the Enzyme Activity—Initially we have used the heteropolymeric template,

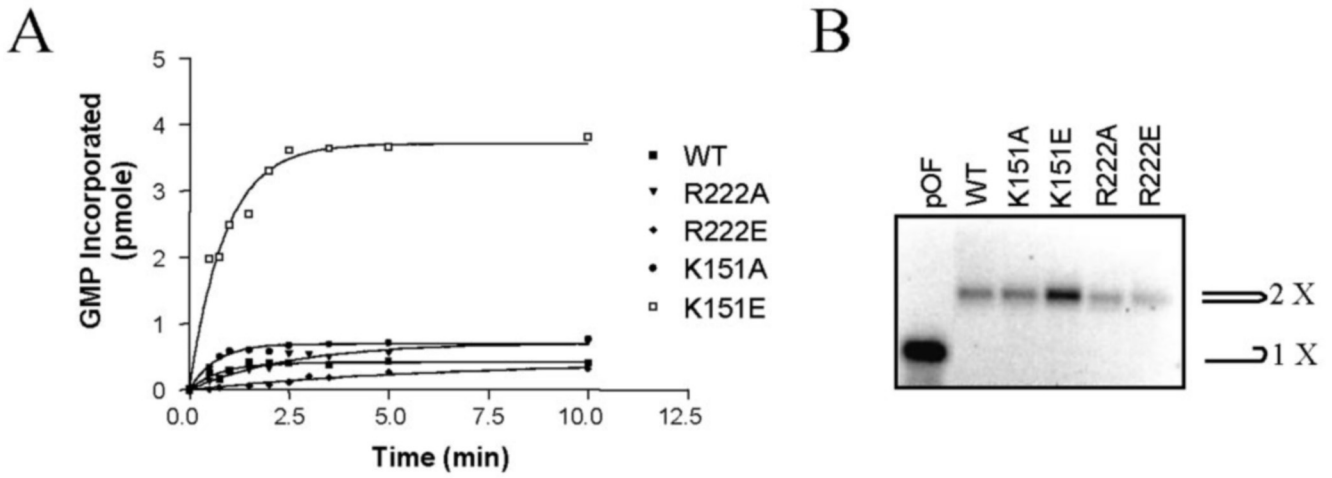

FIG. 7. **Analysis of NS5B mutant activity in a burst assay.** Enzyme (20 nM) was pre-incubated with pOF (20 nM) for 4 h before the addition of the NTP mixture and heparin (800 ng/ml). At each end point, the reaction was stopped by adding 10 μl of EDTA (0.5 M) (*A*) or with an equal volume of phenol:chloroform (1:1) (*B*). In *A*, the nucleotide incorporation was analyzed by DEAE filter binding assay and in *B*, on a 2.5% agarose gel.

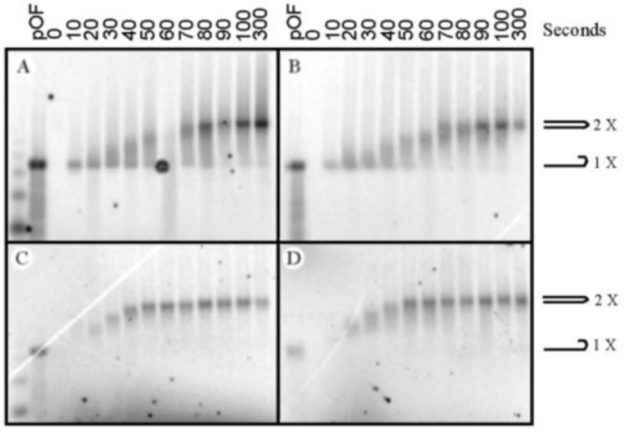

FIG. 8. **Velocity of NTP incorporation in a burst assay.** wt-NS5B (*A* and *C*) and K151E (*B* and *D*) enzymes (20 nM) were pre-incubated with pOF (20 nM) for 4 h before the addition of NTP mixture (100 μM each ATP, CTP, and GTP; 5 μM UTP; and 2.5 μCi of UTP) (*A* and *B*) or 100 μM each ATP, CTP, and UTP; 5 μM GTP; and 2.5 μCi of GTP (*C* and *D*) and heparin (800 ng/ml). At each end point, the reaction was stopped by adding an equal volume of phenol:chloroform (1:1). The incorporation of radioactivity was resolved on a 2.5% agarose gel.

pOF, to examine the K_m values for NTPs of the wt-NS5B enzyme. However, we could not obtain unambiguous K_m values because of the nature of mixed kinetics (biphasic). Therefore, we have chosen homopolymeric templates for subsequent kinetic analyses. To analyze the ability of variant and wild type NS5B enzymes to replicate the RNA templates by *de novo* synthesis, all four homopolymeric templates were tested (poly(A), poly(C), poly(G), and poly(U)). As shown in Table II, only the poly(C) homopolymeric template could be utilized by 20 nM NS5B polymerase under the present conditions. Thus, our data are in agreement with those reported recently for *de novo* initiation of RNA by HCV NS5B (18). The kinetic data for all mutants using poly(C) as template were determined and are summarized in Table II. Interestingly, the nucleotide concentration necessary to initiate *de novo* synthesis is much lower for the K151E mutant (K_m of 118 μM) as compared with the wt-NS5B (K_m of 1096 μM). The markedly higher K_m value (2488 μM) exhibited by R222E is consistent with the notion that this enzyme had a defect in NTP trafficking.

The K_m values obtained for the *de novo* synthesis on these homopolymeric templates reflect an overall K_m that includes the slow process of initiation and the higher rate of elongation. To confirm the increased efficiency of K151E enzyme to initiate *de novo* synthesis, we examined the rate of incorporation of the third and fourth nucleotides using a 23-mer synthetic heteropolymeric RNA (see "Materials and Methods"). The experiment was performed with 1 mM GTP, which represents 1 and 8.5 times the K_m values for the wt-NS5B and K151E enzymes, respectively (Table II). As expected, the K151E enzyme generated more trinucleotide and tetranucleotide products during the first few minutes than the wt-NS5B (data not shown). Taken together, these data suggest that K151E enzyme can utilize more RNA template for *de novo* synthesis when compared with the wt-NS5B under our experimental conditions.

DISCUSSION

It has been well documented that highly purified HCV NS5B polymerase can catalyze complementary RNA synthesis from self-primed or non-primed RNA templates (16–19). Interestingly, the enzyme does not exhibit template specificity, and only a small fraction of the purified protein is catalytically competent (35). In addition, the x-ray-derived crystal structure has revealed elements of the enzyme that might be involved in the dynamics of the multistep reaction pathways (26, 27). Recently, the resolution of the double-stranded RNA polymerase of the bacteriophage ϕ6 revealed unexpected structural similarities with the HCV NS5B enzyme, *i.e.* both enzymes contain a Λ1-loop joining the fingers and the thumb and can initiate *de novo* replication (28). Bressanelli *et al.* (36) further suggested that both enzymes may use very similar mechanism to initiate *de novo* replication. This study reinforces the importance of this structural motif as an integral part of the enzyme function.

The Λ1-loop, spanning amino acids 12–46 of HCV NS5B polymerase, emanates from the fingers to the thumb. This loop forms two α-helical turns and packs closely against helices of the thumb subdomain. Recently, Butcher *et al.* (28) have also identified a similar element from the x-ray derived structure of the ϕ6 RNA-dependent RNA-polymerase, which has a closed conformation as proposed for the NS5B enzyme. Although the exact function of the Λ1-loop is unknown, this loop is likely to be flexible in the absence of a highly structured element and may be engaged in coordinating the "clamping" motion of the enzyme. Based on this premise, we conjectured that removal of the Λ1-loop anchor might perturb the closed conformation of the "active" enzyme leading to an open conformation of an "inactive" enzyme. In the present study, the leucine 30, which

TABLE II
Enzyme parameters using homopolymeric template with or without dinucleotide primer

Enzyme	Poly(C)				Poly(C)/pGG				Poly(A)/pUU			
	K_m[a]	V_{max}[b]	k_{cat}[c]	K_{cat}/K_m[d]	K_m[a]	V_{max}[b]	k_{cat}[c]	K_{cat}/K_m[d]	K_m[a]	V_{max}[b]	k_{cat}[c]	K_{cat}/K_m[d]
NS5B-wt	1096 ± 156	2.9 ± 0.20	2.9 ± 0.20	2673	5.2 ± 0.33	2.3 ± 0.04	2.3 ± 0.04	446,154	117 ± 16	1.2 ± 0.1	1.2 ± 0.1	10,066
K151A	942 ± 103	2.5 ± 0.13	2.5 ± 0.13	2611	4.1 ± 0.69	1.3 ± 0.05	1.3 ± 0.05	309,756	304 ± 84	2.2 ± 0.48	2.2 ± 0.48	7346
K151E	118 ± 10	2.4 ± 0.06	2.4 ± 0.06	21,909	2.6 ± 0.30	1.8 ± 0.05	1.8 ± 0.05	673,077	23 ± 3	1.7 ± 0.09	1.7 ± 0.09	73,913
R222A	1266 ± 240	0.7 ± 0.07	0.7 ± 0.07	585	1.2 ± 0.38	0.7 ± 0.04	0.7 ± 0.04	566,667	NA[e]	NA	NA	NA
R222E	2488 ± 575	2.0 ± 0.29	2.0 ± 0.29	784	12.5 ± 1.04	3.8 ± 1.00	3.8 ± 1.00	304,000	NA	NA	NA	NA

[a] Apparent K_m are in μM.
[b] V_{max} are expressed as picomoles of GMP (poly(C) or poly(C)/pGG) or UMP (poly(A)/pUU) incorporated per minute.
[c] K_{cat} are expressed as min^{-1}, assuming that all enzyme molecules are active.
[d] K_{cat}/K_m are expressed as mol^{-1} min^{-1}.
[e] NA, no activity detected.

has strong hydrophobic interactions with the thumb domain, was substituted for polar residues, a serine or arginine (L30S or L30R). The different chromatographic behavior observed in the elution profile of both L30S and L30R mutants from the heparin column reflects a modification of the charges exposed to the resin, which is highly suggestive of a structural modification of the enzyme. However, the real-time analytical ultracentrifugation experiment indicated that the global shapes of L30S and wt-NS5B proteins are comparable, both being monomeric in solution with sedimentation coefficients of 3.8 and 3.9 S, respectively. During the preparation of this report, two groups have reported that NS5B enzyme can form oligomers in the absence of RNA and this oligomerization property is critical for the enzyme activity (32, 33). These observations are in contrast to our present finding, which clearly shows that the wt-NS5B and L30S mutant enzyme may form higher ordered molecules only in the presence of RNA templates. This discrepancy can be the result of subtle differences in NS5B sequence or sample preparations. Because we were employing a very sensitive and quantitative measurement, *i.e.* the analytical ultracentrifugation to examine the biophysical states of the enzymes in a real-time condition, we are convinced that our purified enzymes are monomeric in solution. However, oligomerization of the enzyme can be induced by RNA binding. The data from analytical ultracentrifugation also suggest that Leu-30 mutation might have rendered the enzyme a local modification at the contact site between the Λ1-loop and the thumb domain because its intrinsic ability of oligomerization in the presence of RNA template is very different from that of the wild type enzyme. A recent study has suggested the implication of the Λ1-loop in the binding of rGTP in an unexpected binding pocket located between the fingers and the thumb (36). Interestingly, the amino acids Glu-18 and His-502, which have been suggested to be important for oligomerization and enzyme activity, are located either in the Λ1-loop (Glu-18) or in the thumb domain spatially close to leucine 30 (His-502) (32). This new observation further supports our notion that the detrimental point mutations of Leu-30 might lead to a local perturbation in the Λ1-loop, which in turn could have: (i) changed the dynamic motion of the finger and thumb domain conferred by the Λ1-loop, (ii) altered the binding of the rGTP, or (iii) reduced or inhibited the proper oligomerization of the enzyme. Currently, we are in the process of determining the essential residue(s) of the protein required for this RNA-induced oligomerization as well as evaluating the effects of this intrinsic biophysical property on RdRP activity. Ultimately, the crystal structure of the L30S will be necessary to unambiguously verify the proposed conformational change provoked by the modification of the leucine 30.

The NS5B polymerase has a cavity called an NTP tunnel leading from the peripheral of the enzyme to the active site. It is conceivable that this tunnel allows efficient trafficking of the nucleotides to the active site. Basic amino acids that are located within the NTP tunnel might play a key role in the trafficking of the incoming NTPs through interaction with the nucleotide phosphate group. Our results suggest that arginine 222 is involved in the NTP trafficking, whereas lysine 151 is dispensable for this function. Because arginine 222 is at close proximity to the active site, its substitution for the glutamic acid should in theory repel any incoming NTPs away from the active site. Indeed, the R222E mutant was completely inactive when the enzyme reaction was carried out at low NTP concentrations. However, only a 2-fold reduction of the enzyme activity was observed with the R222E substitution at high NTP concentration, This latter observation could imply that the NTPs could bypass the requirement of interaction with this residue, or they could possibly use an alternative path to reach the active site. Although there is a possibility of an electrostatic effect of R222E, which may alter the active site, we believe that NTP trafficking plays a key role for the detrimental effect of the R222E mutant based on the following arguments: 1) a higher K_m value for GTP when compared with the wt-NS5B, 2) the fact that this detrimental effect can be reversed by increasing NTP concentration, and 3) the fact that the orientation of the side chain of Arg-222 is gearing away from the active site based on the crystal structure information.

As described previously, the K151E substitution is located away from the active site and on the enzyme surface at the delta of the NTP tunnel. Recently, it has been reported that lysine 151 can form weak electrostatic interaction of 4.3 Å with the triphosphate moiety of the NTP located at the interrogation site (I) of the active site (33). These authors further suggest that this weak interaction is involved in stabilizing the incoming nucleotides transiently for interrogation before it transfers to the priming site (P). Changing lysine 151 for a glutamic acid should still allow a weak interaction through water molecule bridges (5.5 Å) between the amino acid 151 (Glu-151) and the triphosphate moiety. However, the interaction described by Bressanelli *et al*. (36) is solvent-exposed, which weakens the interaction and may not be relevant to explain the enhanced activity of the L151E enzyme. Our data showed that K151E was much more active than wt-NS5B in using a self-primed template for copy-back RNA synthesis at room temperature. However, within linear kinetic parameters, the difference was 2–3-fold at completion of the reaction under optimal conditions at 37 °C. Burst kinetics analyses clearly indicated that K151E can form more pre-initiation complex (7-fold) than the wt-NS5B under single cycle replication. Furthermore, K151E utilizes non-primed RNA templates more efficiently than the wild type enzyme for *de novo* RNA synthesis. It was a surprising finding to observe the enhancement of the K151E enzyme activity. At this point, we do not have an answer to the effect of this point mutation. Interestingly, the lysine 151 is well conserved among the different genotypes of HCV. In addition, human immunodeficiency virus-reverse transcriptase as well as ϕ6 RNA-dependent polymerase possess a counterpart of the

HCV NS5B lysine 151. This observation suggests that the lysine 151 may have a conserved functional role, although our study suggests a regulatory role. One attractive possibility is that lysine 151 could interact with other viral proteins and/or host cell factors involved in HCV replication *in vivo*. Thus, it will be informative to elucidate the function of this K151E substitution in replication of the HCV subgenomic replicon in cells. One can also argue that the superactive K151E enzyme can be exploited for KI determination of small molecule inhibitor. Indeed, searches for small molecule inhibitors by high-throughput screening are usually performed at room temperature where the conditions are far from optimal for the wt-NS5B enzyme.

In summary, we have evaluated the involvement of two structural motifs in NS5B activity *in vitro* based on the structural information derived from its crystal and identified key residues within these structural elements that down and up regulate the enzyme activity. Although our results have provided the first experimental proof of the importance of these structural motifs, the exact mechanism of how the NS5B polymerase catalyzes HCV genome replication in cells is largely unknown. It is very likely that the enzyme exists as a component of a multiprotein complex composed of other viral encoded proteins and/or host factors on membranes of cells to facilitate replication of the HCV genomic RNA. Unlike what is observed *in vitro*, the template specificity and replication efficiency of the NS5B enzyme might be regulated by the components of the complex. Furthermore, the present study also demonstrates for the first time that the NS5B enzyme is monomeric in solution. Further investigation in the intrinsic ability of the enzyme to oligomerize in the presence of RNA template and the biological relevance of this biophysical interaction is warranted.

Acknowledgments—We thank the HCV discovery team at Wyeth for providing pOF substrate, pET-24b/NS5B plasmid, and AT-1 template in this study. We also thank Nathalie Fournier for excellent technical assistance.

REFERENCES

1. Sarbah, S, and Younossi, Z. (2000) *J. Clin. Gastroenterol.* **30,** 125–143
2. World Health Organization. (1998) *Lancet* **351,** 1415
3. Reichard, O., Norkrans, G., Fryden, A., Bracanier, J. H., Sonnerborg, A., Weiland, O., and Swedish Study Group (1998) *Lancet* **351,** 83–87
4. Murphy, F. A., Fauquet, C. M., Bishop, D. H. L., Ghabrial, S. A., Jarvis, A. W., Martelli, G. P., Mayo, M. A., and Summers, M. D. (1995) *Classification and Nomenclature of Viruses: Sixth Report of the International Committee on Taxonomy of Viruses*, pp. 424–426, Springer-Verlag, Vienna
5. Clarke, B. (1997) *J. Gen. Virol.* **78,** 2397–2410
6. Bartenschlager, R. (1997) *Antiviral. Chem. Chemother.* **8,** 281–301
7. Bartenschlager, R., Ahlborn-Laake, L., Mous, J., and Jacobsen, H. (1993) *J. Virol.* **67,** 3835–3844
8. Baumert, T. F., Ito, S., Wong, D. T., and Liang, T. J. (1998) *J. Virol.* **72,** 3827–3836
9. Behrens, S. E., Tomei, L., and De Francesco, R. (1996) *EMBO J.* **15,** 12–22
10. Kim, D. W., Gwack, Y., Han, J. H., and Choe, J. (1995) *Biochem. Biophys. Res. Commun.* **215,** 160–166
11. Lohmann, V., Körner, F., Koch, J. O., Herian, U., Theilmann, L., and Bartenschlager, R. (1999) *Science* **285,** 110–113
12. Ferrari, E., Wright-Minogue, J., Fang, J. W. S., Baroudy, B. M., Lau, J. Y. N., and Hong, Z. (1999) *J. Virol.* **73,** 1649–1654
13. Lohmann, V., Körner, K., Herian, U., and Bartenschlager, R. (1997) *J. Virol.* **71,** 8416–8428
14. Tomei, L., Vitale, R. L., Incitti, I., Serafini, S., Altamura, S., Vitelli, A., and De Francesco, R (2000) *J. Gen. Virol.* **81,** 759–767
15. Yuan, Z. H., Kumar, U., Thomas, H. C., Wen, Y. M., and Monjardino, J. (1997) *Biochem. Biophys. Res. Commun.* **232,** 231–235
16. Oh, J. W., Ito, T., and Lai, M. M. C. (1999) *J. Virol.* **73,** 7694–7702
17. Kao, C. C., Yang, X., Kline, A., Wang, Q. M., Barket, D., and Heinz. B. A., (2000) *J. Virol.* **74,** 11121–11128
18. Luo, G., Hamatake, R. K., Mathis, D. M., Racela, J., Rigat, K. L., Lemm, J., and Colonno, R. J. (2000) *J. Virol.* **74,** 851–863
19. Zhong, W., Uss, A. S., Ferrari, E., Lau, J. Y. N., and Hong, Z. (2000) *J. Virol.* **74,** 2017–2022
20. Blumenthal, T. (1980) *Proc. Natl. Acad. Sci. U. S. A.* **77,** 2601–2605
21. Kao, C. C., Del Vecchio, A. M., and Zhong. W. (1999) *Virology* **253,** 1–7
22. Kao, C. C., and Sun, J. H. (1996) *J. Virol.* **70,** 6826–6830
23. Kim, M. J., Zhong, W., Hong, Z., and Kao, C. C. (2000) *J. Virol.* **74,** 10312–10322
24. Makeyev, E. V., and Bamford, D. H. (2000) *EMBO J.* **19,** 124–133
25. Sun, J. H., Adkins, S., Faurote, G., and Kao, C. C. (1996) *Virology* **226,** 1–12
26. Bressanelli, S., Tomei, L., Roussel, A., Incitti, I., Vitale, R. L., Mathieu, M., De Francesco, R., and Rey, F. A. (1999) *Proc. Natl. Acad. Sci. U. S. A.* **96,** 13034–13039
27. Lesburg, C. A., Cable, M. B., Ferrari, E., Hong, Z., Mannarino, A. F., and Weber, P. C. (1999) *Nat. Struct. Biol.* **6,** 937–943
28. Butcher, S. J., Grimes, J. M., Makeyev, E. V., Bamford, D. H., and Stuart, D. I. (2001) *Nature* **410,** 235–240
29. Hong, Z., Cameron, C. E., Walker, M. P., Castro, C., Yao, N., Lau, J. Y. N., and Zhong, W. (2001) *Virology* **285,** 6–11
30. Schuck, P. (2000) *Biophys. J.* **78,** 1606–1619
31. Qin, W., Yamashita, T., Shirota, Y., Lin, Y., Wei, W., and Murakami, S. (2001) *Hepatology* **33,** 728–737
32. Qin, W., Luo, H., Nomura, T., Hayashi, N., Yamashita, T., and Murakami, S. (2002) *J. Biol. Chem.* **277,** 2132–2137
33. Wang, Q. M., Hockman, M. A., Staschke, K., Johnson, R. B., Case, K. A., Lu, J., Parsons, S., Zhang, F., Rathnachalam, R., Kirkegaard, K., and Colacino, J. M. (2002) *J. Virol.* **76,** 3865–3872
34. Zhong, W., Ferrrari, E., Lesburg, C. A., Maag, D., Ghosh, S. K. B., Cameron, C. E., Lau, J. Y. N., and Hong, Z. (2000) *J. Virol.* **74,** 9134–9143
35. Carroll, S. S., Sardana, V., Yang, Z., Jacobs, A. R., Mizenko, C., Hall, D., Hill, L., Zugay-Murphuy, J., and Kuo, L. C. (2000) *Biochemistry* **39,** 8243–8249
36. Bressanelli, S., Tomei, L., Rey, F. A., and De Francesco, R. (2002) *J. Virol.* **76,** 3482–3492